ISSN 1674-1056
http://cpb.iphy.ac.cn
http://iopscience.iop.org/cpb
中国物理 B
Chinese Physics
中国物理 Chinese Physics B

Tetraalkyl-substituted zinc phthalocyanines used as anode buffer layers for organic light-emitting diodes

Qian Chen(陈潜), Songhe Yang(杨松鹤), Lei Dong(董磊), Siyuan Cai(蔡思源), Jiaju Xu(许家驹), Zongxiang Xu(许宗祥)
Citation: Chin. Phys. B . 2020, 29(1): 017302 . **doi:** 10.1088/1674-1056/ab5933
Journal homepage: http://cpb.iphy.ac.cn; http://iopscience.iop.org/cpb

What follows is a list of articles you may be interested in

Key technologies for dual high-*k* and dual metal gate integration

Yong-Liang Li(李永亮), Qiu-Xia Xu(徐秋霞), Wen-Wu Wang(王文武)
Chin. Phys. B . 2018, 27(9): 097306 . **doi:** 10.1088/1674-1056/27/9/097306

Improved performance of Au nanocrystal nonvolatile memory by N_2-plasma treatment on HfO_2 blocking layer

Chen Wang(王尘), Yi-Hong Xu(许怡红), Song-Yan Chen(陈松岩), Cheng Li(李成), Jian-Yuan Wang(汪建元), Wei Huang(黄巍), Hong-Kai Lai(赖虹凯), Rong-Rong Guo(郭榕榕)
Chin. Phys. B . 2018, 27(6): 067303 . **doi:** 10.1088/1674-1056/27/6/067303

Stress-induced leakage current characteristics of PMOS fabricated by a new multi-deposition multi-annealing technique with full gate last process

Yanrong Wang(王艳蓉), Hong Yang(杨红), Hao Xu(徐昊), Weichun Luo(罗维春), Luwei Qi(祁路伟), Shuxiang Zhang(张淑祥), Wenwu Wang(王文武), Jiang Yan(闫江), Huilong Zhu(朱慧珑), Chao Zhao(赵超), Dapeng Chen(陈大鹏), Tianchun Ye(叶甜春)
Chin. Phys. B . 2017, 26(8): 087304 . **doi:** 10.1088/1674-1056/26/8/087304

Analytical capacitance model for 14 nm FinFET considering dual-*k* spacer

Fang-Lin Zheng(郑芳林), Cheng-Sheng Liu(刘程晟), Jia-Qi Ren(任佳琪), Yan-Ling Shi(石艳玲), Ya-Bin Sun(孙亚宾), Xiao-Jin Li(李小进)
Chin. Phys. B . 2017, 26(7): 077303 . **doi:** 10.1088/1674-1056/26/7/077303

High holding voltage SCR for robust electrostatic discharge protection

Zhao Qi(齐钊), Ming Qiao(乔明), Yitao He(何逸涛), Bo Zhang(张波)
Chin. Phys. B . 2017, 26(7): 077304 . **doi:** 10.1088/1674-1056/26/7/077304

Tetraalkyl-substituted zinc phthalocyanines used as anode buffer layers for organic light-emitting diodes*

Qian Chen(陈潜), Songhe Yang(杨松鹤), Lei Dong(董磊), Siyuan Cai(蔡思源), Jiaju Xu(许家驹)†, and Zongxiang Xu(许宗祥)‡

Department of Chemistry, Southern University of Science and Technology, Shenzhen 518055, *China*

(Received 15 July 2019; revised manuscript received 15 November 2019; accepted manuscript online 20 November 2019)

Two soluble tetraalkyl-substituted zinc phthalocyanines (ZnPcs) for use as anode buffer layer materials in tris(8-hydroxyquinoline)aluminum (Alq_3)-based organic light-emitting diodes (OLEDs) are presented in this work. The hole-blocking properties of these ZnPc layers slowed the hole injection process into the Alq_3 emissive layer greatly and thus reduced the production of unstable cationic Alq_3 (Alq_3^+) species. This led to the enhanced brightness and efficiency when compared with the corresponding properties of OLEDs based on the popular poly-(3, 4-ethylenedioxythiophene): poly(styrene sulfonate) (PEDOT: PSS) buffer layer. Furthermore, because of the high thermal and chemical stabilities of these ZnPcs, a nonaqueous film fabrication process was realized together with improved charge balance in the OLEDs and enhanced OLED lifetimes.

Keywords: organic light-emitting diode, anode buffer layer, metal phthalocyanine, solution process

PACS: 73.40.Qv, 73.90.+f **DOI:** 10.1088/1674-1056/ab5933

1. Introduction

Since they were first reported by Tang and VanSlyke in 1987, multilayer organic light-emitting diodes (OLEDs) have been widely investigated because of their remarkable range of applications in display and lighting technologies. OLEDs offer advantages that include flexibility, large device area, light weight, a solid-state nature, wide viewing angles, fast switching speeds, and low cost.[1–3] Following the significant progress made in both academic and industrial researches over the past three decades, OLED technology is now entering the market. To ensure their widespread commercial application in the future, new material systems and manufacturing process technologies must be developed continuously on an ongoing basis.[4]

Device efficiency and device lifetime, which are the two main concerns for practical use, are directly related to the energy consumption and long-term stability/durability and are largely governed by the charge balance in OLEDs.[5–8] Therefore, to obtain an efficient OLED, it is essential to optimize the charge carrier injection, transport, and recombination processes in the device.[5,6,9] Indium tin oxide (ITO) is the preferred anode material for use in electroluminescent devices because of its high conductivity and high transparency in the visible spectral regime.[9] However, the relatively low work function of ITO together with the interface dipoles that occur at the conventional ITO/organic interfaces typically induce high barriers for hole injection.[4,9] Therefore, insertion of a hole injection layer (HIL) between the ITO anode and the organic hole transport layer (HTL) has become a popular strategy for provision of favorable band alignment in OLEDs.[10–13]

The metal oxides such as WO_3,[14] V_2O_5,[15] MoO_3,[3,13,16–18] ReO_3,[19] and NiO_x[20] are important HIL materials and have been used widely to enhance the hole injection because they offer appropriate energy levels, good thermal stability, and excellent charge carrier mobility.[8] However, these inorganic HILs are usually prepared by annealing a precursor layer at relatively high temperatures, which thus limits the application of these materials in flexible electronic products.[8]

Conducting polymers represent another class of HIL/HTL materials. Their unique optical and electrical properties have allowed them to demonstrate promising potentials for use in flexible optoelectronic devices.[8] Among these materials, poly-(3, 4-ethylenedioxythiophene): poly(styrene sulfonate) (PEDOT: PSS) is one of the most popular HIL/HTL materials because of its appropriate energy levels and ability to form smooth films on ITO substrates.[21,22] Unfortunately, challenges including ITO etching, indium diffusion, water residue, exciton quenching, and weak adhesion still exist.[2,9,23,24] In addition, water residue induced by aqueous PEDOT: PSS dispersion can introduce damage to the devices that typically leads to poor long-term durability.[8,9]

Since the first demonstration of the use of copper phthalocyanine (CuPc) to modify the ITO anode of an OLED by Tang and VanSlyke in 1996,[5] the use of metal phthalocyanines (MPcs) as anode buffer layers has been subject to intensive

*Project supported by the Shenzhen Personal Maker Project, China (Grant No. GRCK2017082316173208), the Shenzhen Overseas High-level Talents Innovation Plan of Technical Innovation, China (Grant No. KQJSCX20180323140712012), and the Special Funds for the Development of Strategic Emerging Industries in Shenzhen, China (Grant No. JCJY20170818154457845).

†Corresponding author. E-mail: xujj@sustech.edu.cn

‡Corresponding author. E-mail: xuzx@sustech.edu.cn

© 2020 Chinese Physical Society and IOP Publishing Ltd

investigation with the aim of achieving higher OLED efficiencies and stabilities.[5,9,10,25–30] In most cases, these MPc layers are fabricated via the vacuum sublimation method because of the poor solubility of typical MPcs in organic solvents.[5,25,30] While vacuum processing eases the fabrication of complex OLED configurations with the desired performance and high reliability on a laboratory scale, this approach is very costly because of the expense of maintaining an ultrahigh vacuum combined with its high energy consumption, high operating temperatures, and huge materials losses.[31,32] Unlike vacuum processing, solution-based processing offers the advantages of low-cost fabrication, compatibility with flexible substrates, and the potential for use in large-scale electronic device production,[31,33] and is thus beneficial for industrial manufacturing applications. Numerous studies have thus been conducted to develop new soluble MPcs, in particular, MPcs that can be functionalized using solubilizing alkyl or alkoxy groups on peripheral or nonperipheral positions in the MPc rings are of considerable interest.[31]

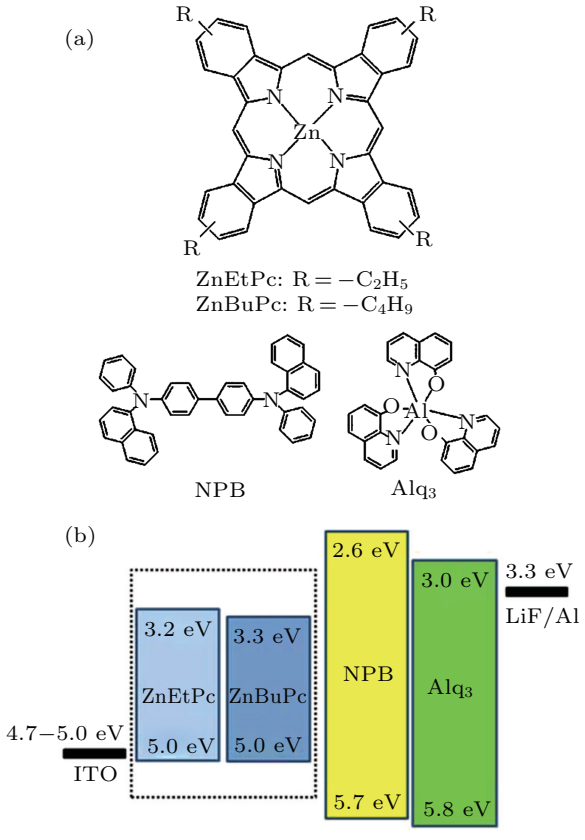


Fig. 1. (a) Molecular structures of the materials used. (b) Device configurations and energy level diagrams of the OLEDs in this study.

In our previous work, we presented two soluble tetraalkyl-substituted copper phthalocyanines (CuEtPc and CuBuPc) that were used as anode buffer layers in OLEDs and when compared with PEDOT: PSS-based OLEDs, enhanced device efficiency and stability were achieved.[9] In this work, we change the central metal in the phthalocyanines from Cu to the less costly Zn and present two soluble tetraalkyl-substituted ZnPcs (ZnEtPc and ZnBuPc, as shown in Fig. 1(a)) for use as anode buffer layers in OLEDs. These ZnPcs demonstrate good solubility in common organic solvents and thus allow the OLED anode buffer layers to be prepared via spin-coating. Typical tris(8-hydroxyquinoline)aluminum (Alq_3)-based OLEDs are fabricated using these layers and characterized to examine the quality of the thin films. The performance and durability of OLEDs containing these ZnEtPc and ZnBuPc buffer layers are also assessed.

2. Experimental details

2.1. Materials

All materials were purchased from Sigma-Aldrich and used without further purification. The ZnEtPc and ZnBuPc (Fig. 1(a)) were synthesized using a method similar to that previously reported in the literature[9,31] and the products were further purified via vacuum sublimation to satisfy the electronic application requirements. The energy levels of ZnPcs were extracted from cyclic voltammetry data and ultraviolet–visible (UV–vis) absorption spectra data using a previously reported method.[34] The highest occupied molecular orbital (HOMO) level for both ZnEtPc and ZnBuPc was determined to be 5.0 eV, which is comparable to that of PEDOT: PSS[8,9,35] and means that these materials are highly suitable for use as OLED anode buffer layers. The energy levels of N, N′-bis-(1-naphthalenyl)-N, N′-bis-phenyl-(1, 1′-biphenyl)-4, 4′-diamine (NPB) and the other OLED materials were obtained from the literature[30] and are summarized in Fig. 1(b).

2.2. Device fabrication and characterization

The device configurations and the corresponding energy level diagrams are illustrated in Fig. 1(b). The OLEDs were fabricated on patterned ITO glass substrates with a sheet resistance of 20 Ω/□. The ZnEtPc/ZnBuPc buffer layers on the ITO substrates were prepared by spin-coating at a rate of 4000 rpm from a ZnEtPc/ZnBuPc solution in dichlorobenzene (10 mg/ml). The thicknesses of the resulting spin-coated layers were measured using a KLA-TENCOR D-100 profiler and were estimated to be approximately 27 nm for both the ZnEtPc and ZnBuPc layers. The other device layers were fabricated by thermal deposition under a pressure of $\sim 1 \times 10^{-6}$ Torr (Mbraun MB200 glovebox). The thicknesses of the vacuum-deposited thin films were monitored *in situ* during deposition using a quartz crystal monitor. All diodes were encapsulated using a UV adhesive in the glovebox (Mbraun MB200) under a N_2 atmosphere prior to the measurements. The emissive area of the as-fabricated OLEDs was 10 mm^2. The current–voltage–luminance characteristics of the OLEDs were recorded using an automated system equipped with a calibrated spectrometer (Photo Research PR680) and a source measurement unit (Keithley 2400). All tests were performed under ambient conditions after the device fabrication and encapsulation.

3. Results and discussion

The hole transport properties of the ZnEtPc and ZnBuPc were examined via top contact field-effect transistor (FET) technology, as shown in Fig. 2. Both the devices using the spin-coated thin films of ZnEtPc and ZnBuPc exhibit a p-type FET behavior, and the charge carrier mobilities of the ZnEtPc and ZnBuPc were determined to be 6.5×10^{-4} cm^2/V·s and 9.5×10^{-4} cm^2/V·s, respectively, which are similar to those of CuEtPc and CuBuPc in our previous work, suggesting that these materials are suitable for the application as anode buffer layers in OLEDs.[9]

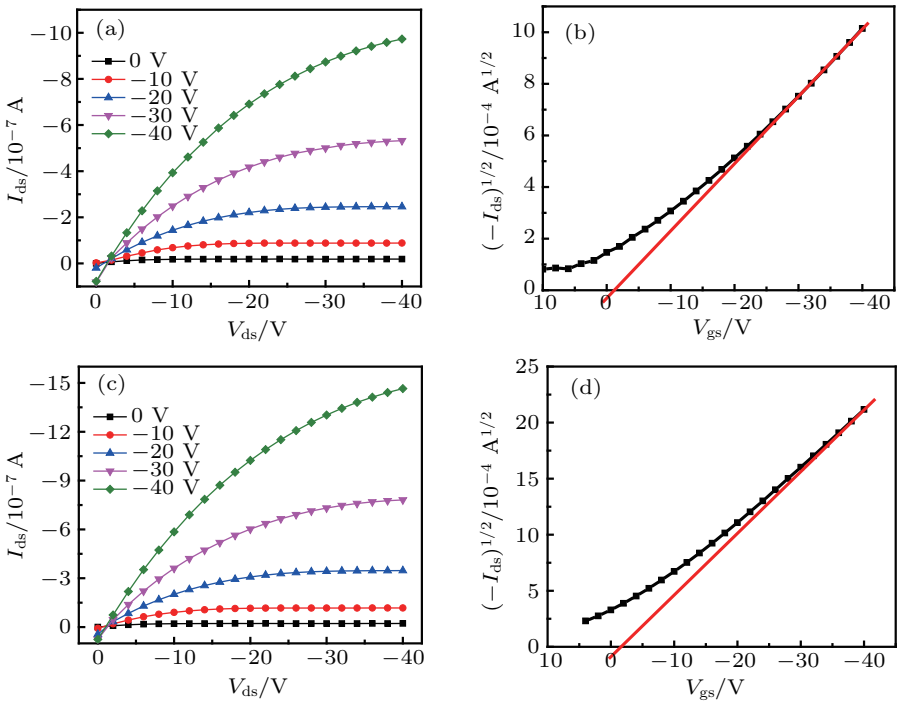


Fig. 2. Output and transfer characteristics of top-contact FETs based on the spin-coating thin films of (a), (b) ZnEtPc and (c), (d) ZnBuPc.

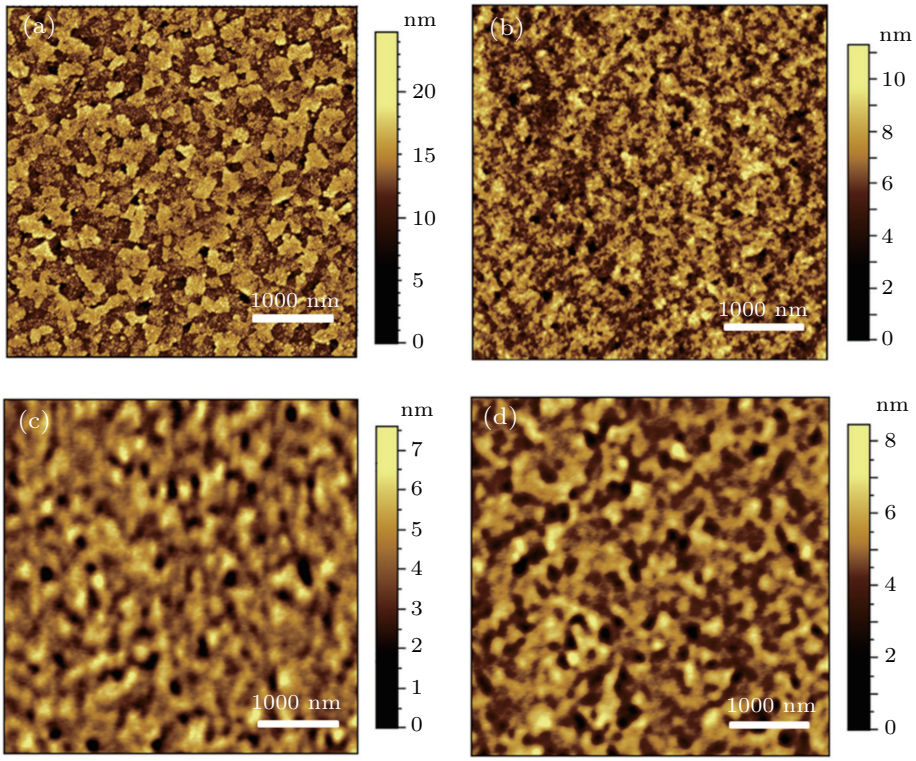


Fig. 3. AFM images of (a) the pristine ITO glass, (b) the PEDOT: PSS film, and the spin-coated thin films of (c) ZnEtPc and (d) ZnBuPc on ITO substrates.

The morphologies of the spin-coated ZnEtPc and ZnBuPc thin films on ITO were studied via atomic force microscopy (AFM) and compared with those of the pristine ITO and the PEDOT: PSS thin film. As shown in Fig. 3, the pristine ITO has a rough surface with a surface root-mean-square (RMS) roughness of 2.36 nm (Fig. 3(a)). The ZnEtPc and ZnBuPc thin films exhibit a smooth and uniform surface characteristic with average surface RMS roughness values of 1.38 nm and 0.92 nm, respectively (Figs. 3(c) and 3(d)), which are similar or lower than that of the PEDOT: PSS thin film (1.29 nm) (Fig. 3(b)). The flat and uniform property of the ZnEtPc and ZnBuPc anode buffer layers between ITO and NPB may help to create a conducting path for charge transport and reduce the pin-hole effect that will affect the long-term durability of OLEDs.

The electroluminescent (EL) spectra of the fabricated OLEDs are shown in Figs. 4(a) and 4(b). Both devices show emission maxima at approximately 530 nm, which is consistent with the EL characteristics of the Alq_3-based OLEDs and indicates that the buffer layers do not cause obvious changes in the emission spectrum of Alq_3.[8,9,25] The transparency spectra of the ZnEtPc and ZnBuPc buffesr are illustrated in Fig. 5, the transparencies of $> 99\%$ and $> 97\%$ at the EL maximum (~ 530 nm) are found for the ZnEtPc and ZnBuPc buffer layers, respectively, indicating that the absorption behavior of these buffer layers has no obvious effect on the EL of the devices.

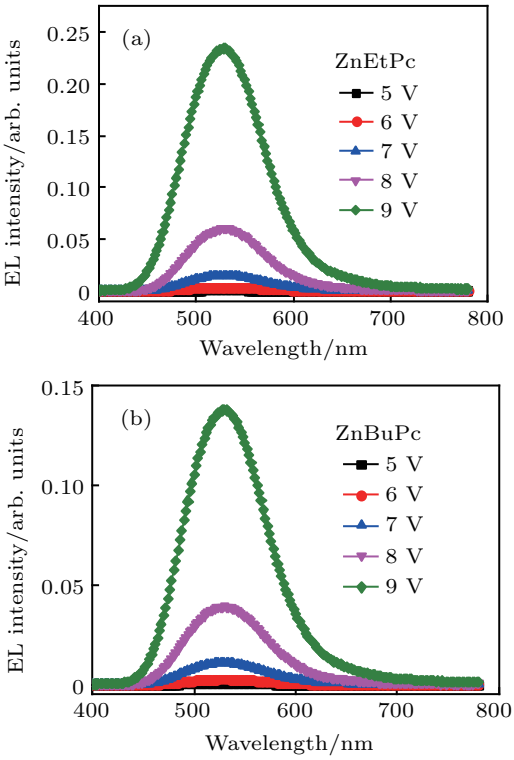


Fig. 4. Electroluminescent spectra of the OLEDs with (a) the ZnEtPc layer and (b) the ZnBuPc layer.

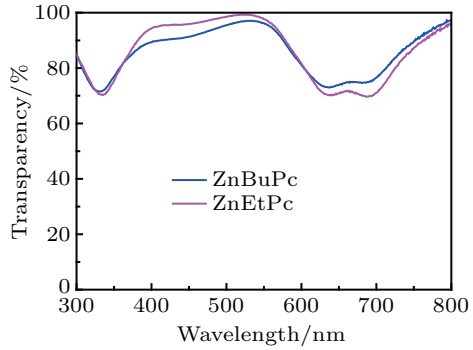


Fig. 5. Transparency spectra of the ZnEtPc and ZnBuPc buffer layers.

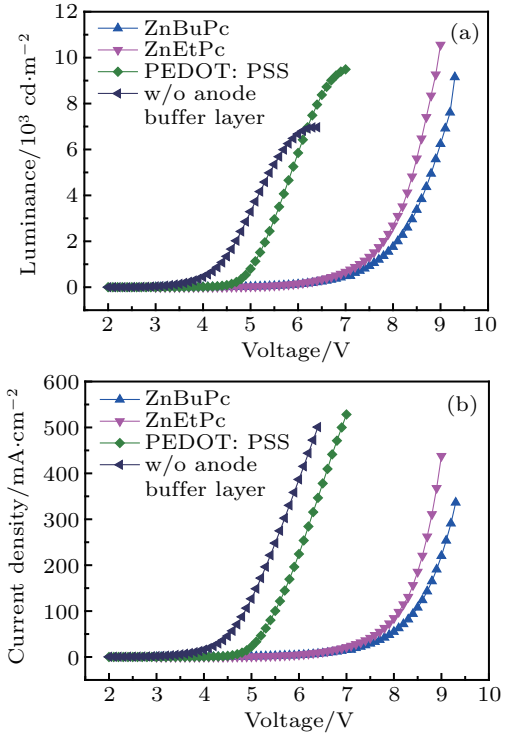


Fig. 6. (a) Luminance–voltage and (b) luminance–current density characteristics of OLEDs. The data for the OLEDs without an anode buffer layer and for those with a PEDOT: PSS layer are taken from the literature.[9]

The luminance–voltage (L–V) and luminance–current density (J–V) curves for all the OLEDs are shown in Figs. 6(a) and 6(b), respectively. When compared with the OLED without the anode buffer layer,[9] the insertion of the ZnEtPc and ZnBuPc interlayers between the ITO and the HTL causes the L–V characteristics to shift toward a higher voltage. Turn-on voltages of 3.7 V and 3.8 V are observed for the OLEDs that contain the ZnEtPc and ZnBuPc buffer layers, respectively, while that of the diode with the single HTL is only 2.5 V, thus indicating that the anode buffer layers impede hole injection into the HTL.[6,7,9] This hole-blocking characteristic is possibly caused by the alkyl groups (i.e., ethyl and butyl) on the ZnPc structures, which form thin "insulating layers" at both the ITO/ZnEtPc (ZnBuPc) and ZnEtPc (ZnBuPc)/NPB interfaces.[9,35] As shown in Table 1, a significant OLED luminance enhancement when compared with that of

the single HTL diode is achieved by inserting the ZnEtPc (ZnBuPc) buffer layer at the ITO/NPB interface. Both ZnPc-based OLEDs exhibit a luminance maximum similar to that of the PEDOT: PSS-based OLED, while the highest luminescence among all the diodes of 10560 cd/m^2 is found for the ZnEtPc-based OLED (Table 1). It was previously reported that hole migration into the Alq_3 layer in Alq_3-based OLEDs led to a reduced fluorescence quantum yield caused by the degradation products of the unstable cationic Alq_3 species (Alq_3^+), which acted as fluorescence quenchers.[6,7,36] The higher brightness of these devices is therefore attributed to the effect of the ZnEtPc and ZnBuPc buffer layers in achieving more balanced hole and electron injection processes by impeding hole injection into the NPB layer.[6,7,9,35,37,38]

Table 1. OLED performance.

Anode buffer layer	$\lambda^{a}_{EL,max}$/nm	CIE^{b} (x, y)	$V^{c}_{turn-on}$/V	LE$^{d}_{max}$/cd·A^{-1}	PE$^{e}_{max}$/lm·W^{-1}	L^{f}_{max}/cd·m^{-2}
W/o anode buffer layer	530	0.313, 0.541	2.5	2.96	2.04	6966
PEDOT: PSS	530	0.314, 0.533	3.0	3.77	1.97	9477
ZnEtPc	530	0.285, 0.544	3.7	3.19	1.31	10560
ZnBuPc	530	0.289, 0.547	3.8	3.22	1.27	9152

[a]Maximum peak value of EL spectrum. [b]Measured at maximum luminance. [c]Turn-on voltage recorded at luminance of 1 cd/m^2. [d]Maximum luminous efficiency. [e]Maximum power efficiency. [f]Maximum luminance. The data for the OLEDs without the anode buffer layer and with the PEDOT: PSS are taken from the literature.[9]

The enhanced charge balance achieved when using the ZnEtPc and ZnBuPc anode buffer layers can also be observed in the luminance–current density (L–J) and current efficiency–current density characteristics (Figs. 7(a) and 7(b), respectively). The luminance increases almost linearly with increasing current density from a low initial current density (approximately 0–100 mA/cm^2) and when the current density exceeds 100 mA/cm^2, a significant roll-off effect can be observed in both diodes, thus indicating the reduced charge balance in the device at high current densities (Fig. 7(a)). Possible causes include exciton–exciton interactions, exciton–charge carrier interactions, and exciton dissociation when the device is operating at a high current density.[8,9,25,39–41] More serious roll-off effects were observed in the single HTL diode and the PEDOT: PSS-based diode, indicating that the ZnEtPc and ZnBuPc layers can significantly optimize both charge carrier injection and transport processes in the OLEDs.[8,9,35] These results are consistent with the characterization results for the current efficiency–current density characteristics, in which the EL efficiencies of all diodes see a sharp rise, thus achieving their maximum values at low current densities, and these efficiencies then decay with increasing current density in the high current density range (Fig. 7(b)). While the PEDOT: PSS-based OLED produces the highest maximum efficiency of 3.77 cd/A at a low current density, the device shows a more obvious efficiency roll-off than that of the OLEDs containing the ZnEtPc and ZnBuPc buffer layers (Fig. 7(b)). The ZnEtPc- and ZnBuPc-based OLEDs generally demonstrate superior EL efficiencies when compared with those of the other two device structures within the main measurement range. It was previously reported that the improved hole impedance into NPB produced by the use of a hole-blocking layer can help to increase the electron density in the Alq_3 layer zone adjacent to the NPB/Alq_3 interface, thus reducing the Alq_3^+ population and improving direct hole injection from the NPB into the anionic Alq_3 species (Alq_3^-) to generate more excited states.[6,9] Similar to the results reported in our previous work,[9] the hole-blocking characteristics of the ZnEtPc and ZnBuPc buffer layers produce better charge balance in the OLEDs, thus giving rise to the improved device performances.[6,7,9,35,38,42]

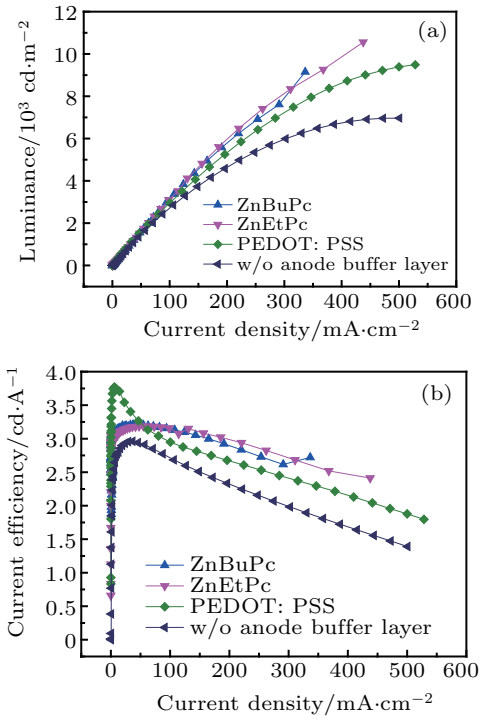


Fig. 7. (a) Luminance–current density and (b) current efficiency–current density characteristics of the four types of OLEDs. The data for the OLEDs without an anode buffer layer and with the PEDOT: PSS buffer layer are taken from the literature.[9]

It can be found that the CIE coordinate value at the OLED maximum luminance undergoes a slight change due to the insertion of the PEDOT: PSS thin film, and a relatively significant alteration when the ZnEtPc and ZnBuPc thin films are

introduced. And similar CIE coordinate values can be found for the ZnEtPc- and ZnBuPc-based OLEDs (Table 1). According to the *L*–*V* and *J*–*V* characteristics of the OLEDs (Fig. 6), all the anode buffer layers exhibit a hole-blocking property for hole injection from the ITO anode, resulting in the enhanced operating voltages compared with the OLED without anode buffer layer. And higher operating voltages of the ZnEtPc- and ZnBuPc-based OLEDs than that of the PEDOT: PSS-based device can be found. It was reported that the recombination zone shifts to the anode side with increased applied voltages, which results in the change of chrominance in the multilayer devices.[43] Thus, the variation in the CIE coordinate is attributed to higher operating voltages due to the hole-blocking properties of these anode buffer layers, which lead to the movement of the recombination zone away from the cathode side and closer to the anode side.

To investigate the effects of the quality of the ZnEtPc and ZnBuPc layers and that of the enhanced charge balance on the long-term device durability, the OLED lifetimes were tested under a constant drive current density of 100 mA/cm^2. As shown in Fig. 8, the OLED lifetimes are significantly improved when using the ZnEtPc and ZnBuPc buffer layers. The luminance of the single HTL diode decays rapidly, showing a poor half-lifetime of 355 min.[9] The OLED lifetime is improved by the insertion of the PEDOT: PSS layer and this OLED exhibits a half-lifetime of 619 min.[9] Significant enhancements in device durability are observed for the OLEDs with the ZnEtPc and ZnBuPc layers, which have half-lifetimes as long as 2245 min and 2367 min, respectively.

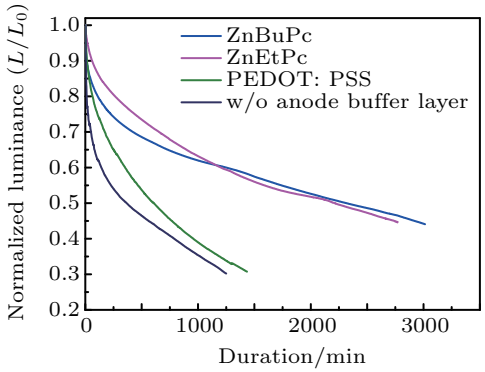


Fig. 8. (a) Normalized luminance vs. operating time characteristics of the OLEDs at a constant current density of 100 mA/cm^2. The data for the OLEDs without an anode buffer layer and with the PEDOT: PSS buffer layer are taken from the literature.[9]

These results reveal the strong correlation between the hole injection and transport processes and the device lifetime.[9,35,41] Indeed, the hole-blocking properties of the ZnEtPc and ZnBuPc anode buffer layers can help to drive the recombination zone away from the cathode, which leads to increased electron density at the NPB/Alq_3 interface and reduced production of the unstable Alq_3^+ species and thus results in longer OLED lifetimes.[6,35,41]

Another factor that is responsible for the increased OLED durability under continuous operation conditions is the quality of the anode buffer layers. It was previously reported that the chemical reaction of PEDOT: PSS with the ITO layer induces instability in ITO/PEDOT: PSS system that typically accelerates the device degradation.[35,44,45] This process can occur during both OLED fabrication and device operation[35,44] and the degradation becomes more serious when the device is exposed to moisture because large amounts of indium can then diffuse further into the neighboring layers and accelerate the degradation of these layers.[9,35,44] Furthermore, because the reaction between Alq_3 and any trace water is believed to be another major failure pathway for Alq_3-based OLEDs,[46] any potential water residue in an OLED induced by aqueous PEDOT: PSS dispersion after fabrication would introduce this danger to the device.[9] Unlike PEDOT: PSS, which is acidic, the ZnEtPc and ZnBuPc layers are highly chemically and thermally stable and thus offer effective protection to the ITO anode. In addition, the spin-coated ZnEtPc and ZnBuPc layers are fabricated from nonaqueous organic solvents (in this work, dichlorobenzene) that can suppress water damage to the device and thus play a role in retarding device degradation.[8,9,35]

4. Conclusions

In summary, two soluble tetraalkyl-substituted ZnPcs (ZnEtPc and ZnBuPc) for use as anode buffer layers in OLEDs are presented. The hole-blocking properties of these ZnPc layers significantly impede hole injection into the Alq_3 emissive layer and thus reduce generation of the unstable Alq_3^+ species, which leads to enhanced OLED luminance and efficiency when compared with the corresponding properties of PEDOT: PSS-based OLEDs. The high thermal and chemical stabilities of these ZnPcs, the nonaqueous ZnPc film fabrication processes, and the enhanced charge balance in the resulting OLEDs lead to the enhancement of the OLEDs' durability. The results of this study indicate a promising direction to follow in future work.

References

[1] Tang C W and VanSlyke S A 1987 *Appl. Phys. Lett.* **51** 913
[2] So F and Kondakov D 2010 *Adv. Mater.* **22** 3762
[3] Xie G, Meng Y, Wu F, Tao C, Zhang D, Liu M, Xue Q, Chen W and Zhao Y 2008 *Appl. Phys. Lett.* **92** 093305
[4] Roy C K, Jaewon L, Neetu C, Alok G, Xuezhong J, Fabrice A and Franky S 2009 *Adv. Funct. Mater.* **19** 491
[5] Slyke S A V, Chen C H and Tang C W 1996 *Appl. Phys. Lett.* **69** 2160
[6] Aziz H, Popovic Z D, Hu N X, Hor A M and Xu G 1999 *Science* **283** 1900
[7] Aziz H and Popovic Z D 2004 *Chem. Mater.* **16** 4522
[8] Feng Y, Xu J, Shan H, Dong L, Sun X, Hu Q, Wang Y, Roy V A L and Xu Z X 2017 *Org. Electron.* **51** 257
[9] Xu J, Wang Y, Chen Q, Lin Y, Shan H, Roy V A L and Xu Z 2016 *J. Mater. Chem. C* **4** 7377
[10] Lee H, Lee J, Yi Y, Cho S W and Kim J W 2015 *J. Appl. Phys.* **117** 035503

[11] Jou J H, Kumar S, Agrawal A, Li T H and Sahoo S 2015 *J. Mater. Chem. C* **3** 2974

[12] Choi Y J, Gong S C, Kang K M and Park H H 2014 *J. Mater. Chem. C* **2** 8344

[13] Liu R, Xu C, Biswas R, Shinar J and Shinar R 2011 *Appl. Phys. Lett.* **99** 093305

[14] Meyer J, Hamwi S, Bülow T, Johannes H H, Riedl T and Kowalsky W 2007 *Appl. Phys. Lett.* **91** 113506

[15] Zhu X L, Sun J X, Peng H J, Meng Z G, Wong M and Kwok H S 2005 *Appl. Phys. Lett.* **87** 153508

[16] Zhu Y K, Zhong J, Lei S Y, Chen H, Shao S S and Lin Y 2017 *Chin. Phys. B* **26** 087302

[17] Mu X, Wu X M, Hua Y L, Jiao Z Q, Shen L Y, Su Y J, Bai J J, Bi W T, Yin S G and Zheng J J 2013 *Chin. Phys. B* **22** 027805

[18] Zhang L, Zhou D Y, Wang B, Shi X B, Hu Y, Wang Z K and Liao L S 2016 *Appl. Phys. Lett.* **109** 173302

[19] Leem D S, Park H D, Kang J W, Lee J H, Kim J W and Kim J J 2007 *Appl. Phys. Lett.* **91** 011113

[20] Chan I M, Hsu T Y and Hong F C 2002 *Appl. Phys. Lett.* **81** 1899

[21] Cook J H, Al-Attar H A and Monkman A P 2014 *Org. Electron.* **15** 245

[22] Roman L S, Mammo W, Pettersson L A A, Andersson M R and Inganäs O 1998 *Adv. Mater.* **10** 774

[23] Kim J S, Friend R H, Grizzi I and Burroughes J H 2005 *Appl. Phys. Lett.* **87** 023506

[24] Wong K W, Yip H L, Luo Y, Wong K Y, Lau W M, Low K H, Chow H F, Gao Z Q, Yeung W L and Chang C C 2002 *Appl. Phys. Lett.* **80** 2788

[25] Wang Y L, Xu J J, Lin Y W, Chen Q, Shan H Q, Yan Y, Roy V A L and Xu Z X 2015 *AIP Adv.* **5** 107205

[26] Mori T, Mitsuoka T, Ishii M, Fujikawa H and Taga Y 2002 *Appl. Phys. Lett.* **80** 3895

[27] Guo R D, Yue S Z, Wang P, Chen Y, Zhao Y and Liu S Y 2013 *Chin. Phys. B* **22** 0127304

[28] Qiu Y, Gao Y, Wei P and Wang L 2002 *Appl. Phys. Lett.* **80** 2628

[29] Chen S F and Wang C W 2004 *Appl. Phys. Lett.* **85** 765

[30] Deng Z, Lü Z, Chen Y, Yin Y, Zou Y, Xiao J and Wang Y 2013 *Solid-State Electron.* **89** 22

[31] Xu J, Wang Y, Shan H, Lin Y, Chen Q, Roy V A L and Xu Z 2016 *ACS Appl. Mater. Interfaces* **8** 18991

[32] Wang Y, Shan H, Sun X, Dong L, Feng Y, Hu Q, Ye W, Roy V A L, Xu J and Xu Z X 2018 *Org. Electron.* **55** 15

[33] Shaoqiang D, Hongkun T, Lizhen H, Jidong Z, Donghang Y, Yanhou G and Fosong W 2011 *Adv. Mater.* **23** 2850

[34] Hong W, Sun B, Aziz H, Park W T, Noh Y Y and Li Y 2012 *Chem. Commun.* **48** 8413

[35] Zheng L, Xu J, Feng Y, Shan H, Fang G and Xu Z X 2018 *J. Mater. Chem. C* **6** 11471

[36] Luo Y, Aziz H, Popovic Z D and Xu G 2007 *J. Appl. Phys.* **101** 034510

[37] Tadayyon S M, Grandin H M, Griffiths K, Norton P R, Aziz H and Popovic Z D 2004 *Org. Electron.* **5** 157

[38] Vestweber H and Rieß W 1997 *Synth. Met.* **91** 181

[39] Hwang J, Choi H K, Moon J, Kim T Y, Shin J W, Joo C W, Han J H, Cho D H, Huh J W, Choi S Y, Lee J I and Chu H Y 2012 *Appl. Phys. Lett.* **100** 133304

[40] Kalinowski J, Stampor W, Mężyk J, Cocchi M, Virgili D, Fattori V and Di Marco P 2002 *Phys. Rev. B* **66** 235321

[41] Kalinowski J, Stampor W, Szmytkowski J, Virgili D, Cocchi M, Fattori V and Sabatini C 2006 *Phys. Rev. B* **74** 085316

[42] Anderson J D, McDonald E M, Lee P A, Anderson M L, Ritchie E L, Hall H K, Hopkins T, Mash E A, Wang J, Padias A, Thayumanavan S, Barlow S, Marder S R, Jabbour G E, Shaheen S, Kippelen B, Peyghambarian N, Wightman R M and Armstrong N R 1998 *J. Am. Chem. Soc.* **120** 9646

[43] Hao J, Deng Z and Yang S 2006 *Displays* **27** 108

[44] Nguyen T P and de Vos S A 2004 *Appl. Surf. Sci.* **221** 330

[45] Cacialli F, Kim J S, Brown T M, Morgado J, Granström M, Friend R H, Gigli G, Cingolani R, Favaretto L, Barbarella G, Daik R and Feast W J 2000 *Synth. Met.* **109** 7

[46] Knox J E, Halls M D, Hratchian H P and Bernhard Schlegel H 2006 *Phys. Chem. Chem. Phys.* **8** 1371